Published in final edited form as:
Dev Biol. 2012 February 15; 362(2): 230–241. doi:10.1016/j.ydbio.2011.12.010.

Analysis of Sphingosine-1-phosphate signaling mutants reveals endodermal requirements for the growth but not dorsoventral patterning of jaw skeletal precursors

Bartosz Balczerski[1,‡], **Megan Matsutani**[1,‡], **Pablo Castillo**[1], **Nick Osborne**[2,3], **Didier Y.R. Stainier**[2], and **J. Gage Crump**[1,*]

[1]Eli and Edythe Broad Institute for Regenerative Medicine and Stem Cell Research, Department of Cell and Neurobiology, University of Southern California Keck School of Medicine, Los Angeles, CA 90033, USA

[2]Department of Biochemistry and Biophysics, University of California, San Francisco, CA 94143, USA

Abstract

Development of the head skeleton involves reciprocal interactions between cranial neural crest cells (CNCCs) and the surrounding pharyngeal endoderm and ectoderm. Whereas elegant experiments in avians have shown a prominent role for the endoderm in facial skeleton development, the relative functions of the endoderm in growth versus regional identity of skeletal precursors have remained unclear. Here we describe novel craniofacial defects in zebrafish harboring mutations in the Sphingosine-1-phospate (S1P) type 2 receptor (*s1pr2*) or the S1P transporter Spinster 2 (*spns2*), and we show that S1P signaling functions in the endoderm for the proper growth and positioning of the jaw skeleton. Surprisingly, analysis of *s1pr2* and *spns2* mutants, as well as *sox32* mutants that completely lack endoderm, reveals that the dorsal-ventral (DV) patterning of jaw skeletal precursors is largely unaffected even in the absence of endoderm. Instead, we observe reductions in the ectodermal expression of Fibroblast growth factor 8a (Fgf8a), and transgenic misexpression of Shha restores *fgf8a* expression and partially rescues the growth and differentiation of jaw skeletal precursors. Hence, we propose that the S1P-dependent anterior foregut endoderm functions primarily through Shh to regulate the growth but not DV patterning of zebrafish jaw precursors.

Keywords

Sphingosine-1-phosphate; Pharyngeal Endoderm; Facial Ectoderm; Craniofacial Skeleton; Shh; Zebrafish

[*]Corresponding author: gcrump@usc.edu, 323-442-2693 (ph), 323-442-4040 (fax).
[‡]These authors contributed equally to this work
[3]Present address: Department of Genetics, University of North Carolina, Chapel Hill, NC 27599, USA

Supplementary materials related to this article can be found online at xxxxxxxxxx.

INTRODUCTION

Reciprocal interactions between epithelia and mesenchyme control the development of many vertebrate organs. In the face, signaling from the adjacent ectodermal and endodermal epithelia helps pattern the CNCC-derived mesenchyme into distinctly shaped cartilages and bones. In particular, Fgf8 from the oral ectoderm (Tucker et al., 1999) and Edn1 and Bmp4 from the more posterior aboral ectoderm (Barlow and Francis-West, 1997) are critical for the growth and regional patterning of the jaw skeleton. Specific deletion of Fgf8 (Trumpp et al., 1999) or Bmp4 (Liu et al., 2005) in the oral ectoderm results in severe reduction of the lower jaw in mice. Similarly, zebrafish and mouse *edn1* mutants display loss or transformation of the lower jaw (Kurihara et al., 1994; Miller et al., 2000), and mosaic experiments in zebrafish have defined the facial ectoderm as a critical source of Edn1 ligand (Nair et al., 2007).

In addition to the ectoderm, the pharyngeal endoderm plays a major role in development of the facial skeleton. Explant studies in newts have demonstrated that pharyngeal endoderm is sufficient to induce chondrogenesis in CNCCs (Epperlein and Lehmann, 1975). In zebrafish, loss of the endoderm in *sox32* (*casanova*) and *bonnie and clyde* mutants leads to an absence of the CNCC-derived craniofacial skeleton, with the exception of the anterior-most neurocranial skull base (Alexander et al., 1999; David et al., 2002; Kikuchi et al., 2001). In avians, ablation and graft experiments have demonstrated that specific domains of foregut endoderm, defined along the anterior-posterior and DV axes, control the formation and even the orientation of distinct facial skeletal elements (Couly et al., 2002; Ruhin et al., 2003). Recent data suggest that the pharyngeal endoderm functions in part through Shh to regulate signaling factor expression in the overlying facial ectoderm (Haworth et al., 2004). Shh is expressed in the early pharyngeal endoderm (Brito et al., 2006), and conditional deletion of the Shh receptor Smoothened in CNCCs results in a near complete absence of the craniofacial skeleton in mice (Jeong et al., 2004). Surgical removal of the anterior head, which includes the Shh-expressing endoderm, results in loss of the lower jaw in avians and can be rescued by Shh beads (Brito et al., 2006). In addition, electroporation of Shh or implantation of Shh-expressing cells in avians induces ectopic lower-jaw-like structures and ectopic expression of *Fgf8*, *Shh*, and *Bmp4* in the facial ectoderm (Brito et al., 2008; Haworth et al., 2007). Whereas the endoderm clearly plays a pivotal role in craniofacial development, the relative requirements of endodermal signals in the growth (i.e. survival and proliferation) versus regional identity of CNCC-derived jaw skeletal precursors is not well understood. By studying zebrafish S1P signaling mutants, as well as *sox32* mutants that lack all endoderm, here we demonstrate that the endoderm is not required for the early DV patterning of jaw skeletal precursors but instead plays a major role in their later growth and/or differentiation. Moreover, we show that Shha misexpression partially rescues the jaw skeleton, *fgf8a* expression, and CNCC growth defects of *sox32* mutants, suggesting that, as in avians, endoderm-derived Shh is critical for jaw development in zebrafish.

Particular domains of endoderm are required for the development of particular skeletal elements in avians (Couly et al., 2002; Ruhin et al., 2003), and we have shown that first pouch endoderm is specifically required for development of dorsal hyoid-arch-derived cartilage in zebrafish (Crump et al., 2004). Here we demonstrate that mutants for the S1P type 2 receptor (*s1pr2*/*miles apart*) and the phospholipid transporter Spinster2 (*spns2*/*two-of-hearts*) have specific defects in the mandibular-arch-derived jaw skeleton. S1P is a phospholipid implicated in cell-cell signaling, with S1P signaling mediating cell migration and morphogenesis in a variety of contexts (reviewed in (Spiegel et al., 2002)). Previous reports in zebrafish have shown that Spinster2 is required in the yolk syncitial layer to transport S1P out of cells (Kawahara et al., 2009; Osborne et al., 2008), whereas the S1pr2 receptor is required in the endoderm for heart development (Kupperman et al., 2000;

Osborne et al., 2008). Both *s1pr2* and *spns2* mutants display disorganization of the anterior-most pharyngeal endoderm, with endoderm defects indirectly affecting medial migration of the lateral plate mesoderm that will form the myocardium (Kupperman et al., 2000; Osborne et al., 2008). Here we use transplantation rescue experiments to demonstrate that the function of S1P signaling in jaw development is to promote the earlier morphogenesis of the anterior-most pharyngeal endoderm, which in turn induces signaling factor expression in the facial ectoderm required for jaw growth.

MATERIALS AND METHODS

Zebrafish Lines and Heat-Shock Treatments

Zebrafish (*Danio rerio)* embryos were raised at 28.5°C and staged as described (Kimmel et al., 1995). Published lines include *spns2* ^{sk12} (Osborne et al., 2008), *s1pr2*^{m93} (Kupperman et al., 2000), *sox32*^{ta56} (Kikuchi et al., 2001), *Tg(~3.4her5:EGFP)*^{ne1911} (Tallafuss and Bally-Cuif, 2003), *Tg(fli1a:EGFP)*^{y1} (Lawson and Weinstein, 2002), and *Tg(hsp70I:Gal4)*$^{kca4/+}$ (Scheer and Campos-Ortega, 1999). The Gateway Tol2kit (Kwan et al., 2007) was used to construct *UAS*:Shha fish. The zebrafish *shha* cDNA was amplified with primers Shha-1F: GGGGACAAGTTTGTACAAAAAAGCAGGCTCGGCCACCATGCGGCTTTTGACGAGAG T and Shha-2R: GGGGACCACTTTGTACAAGAAAGCTGGGTTCAGCTTGAGTTTACTGACA and inserted into pDONR221 to create pME-Shha. p5E-UAS, pME-Shha, p3E-pA, and pDestTol2CG2 were combined to create *UAS*:Shha:pA, *cmlc2*:GFP, which was injected with Transposase RNA into one-cell-stage embryos. Based on *cmlc2*:GFP heart fluorescence, two independent lines were isolated (*el106* and *el137*). *Tg(hsp70I:Gal4)*$^{kca4/+}$; *Tg(UAS:Shha:pA, cmlc2:GFP)*^{el137} embryos were subjected to heat-shock treatment in a 40°C incubator from 14.5–16.5 hours-post-fertilization (hpf). *UAS*:Shha embryos were selected for heart GFP, and genotyping confirmed *hsp70I*:Gal4 (Zuniga et al., 2010). *hsp70I*:Gal4-negative siblings were used as controls. To construct *sox10*:kikGR fish, the ~4.9 kb *sox10* promoter (Carney et al., 2006) was amplified with primers Sox10L: GGGGACAACTTTGTATAGAAAAGTTGCAGAACTGCTTTTTGTTCCTCA and Sox10R: GGGGACTGCTTTTTTGTACAAACTTGGCCACAGGTGACTTCGGTA and inserted into pDONR-p4p1R to create p5E-Sox10. The kikGR cDNA (MBL International) was amplified using primers KikGR-L: GGGGACAAGTTTGTACAAAAAAGCAGGCTCCACCATGGTGAGCGTGATCACCAG and KikGR-R: GGGGACCACTTTGTACAAGAAAGCTGGGTCTACTTGGCCAGCCTGGGCAGGC and inserted into pDONR221 to create pME-KikGR. p5E-Sox10, pME-KikGR, p3E-pA, and pDestTol2pA2 were combined to create *sox10*:kikGR:pA, which was injected with Transposase RNA into one-cell-stage embryos, and stable line *Tg(~4.9sox10:kikGR)*^{el2} was used for further analysis.

Identification of the *toh*^{b1110} mutant

From a parthenogenic diploid F2 screen (Miller et al., 2004), we isolated the *spns2*^{b1110} allele based on Meckel's cartilage defects. The lesion changes A to T at nucleotide 427 of the *spns2* cDNA, which creates a DdeI site (lowercase shows mutation: ACCtAAGAA). Genotyping was performed with primers tohIDL: AATCTTTTTCTGGTCCGCTGT and tohIDR: ACCAATGCAAACCTTTCTGG. Digestion with DdeI generates nucleotide bands of 182/29 in wild types and 165/29/17 in mutants.

In Situ Hybridization, Skeletal Analysis, and Cell Proliferation and Death Assays

Two-color acid-free skeletal staining with Alcian Blue and Alizarin Red (Walker and Kimmel, 2007) and in situ hybridizations (Zuniga et al., 2010) were performed as described. Previously published probes include *fgf8a* (Maves et al., 2002) and *dlx2a*, *hand2*, *dlx3b*, *msxe*, and *jag1b* (Zuniga et al., 2010). *shha*, *pitx2ca*, *edn1*, and *bmp4* probes were synthesized with T7 RNA polymerase from PCR products amplified from 6 dpf zebrafish genomic DNA with the following primers: Shha-L: GACACCTCTCGCCTACAAGC, Shha-R: GCTAATACGACTCACTATAGGCGAGGACAAAAAGGAGGTGA, Pitx2ca-L: TCCCAGACCATGTTCTCTCC, Pitx2ca-R: GCTAATACGACTCACTATAGGTCGCAAGCAAGACATGATTC, Edn1-L: GGAAACGCTCCACGTAAGAA, Edn1-R: GCTAATACGACTCACTATAGGTTGGTTTGGATGAAGGCAAT, Bmp4-L: GACACCTCTCGCCTACAAGC, and Bmp4-R: GCTAATACGACTCACTATAGGCGTAGCTGGTCCCACTCTTC. Genotyping of embryos confirmed all phenotypes. For cell death assays, LysoTracker Red DND-99 (Invitrogen) was diluted to 5 μM in Embryo Media. Embryos were manually dechorionated and incubated with LysoTracker in the dark for 45 minutes at 28.5°C. After 4–5 washes in Embryo Media, embryos were fixed in 4% paraformaldehyde in PBS, rocked at 4°C overnight, washed once with PBT, dehydrated and rehydrated in methanol, and viewed in PBT. For anti-phosphohistone H3 (pH3) staining, embryos were fixed in 4% PFA overnight at 4°C, washed for 5 minutes in PBS, 5 minutes in H_2O, 12 minutes in cold acetone, and 5 minutes in H_2O. Embryos were then rehydrated into PBS, rinsed for 15 minutes in PBDTx, blocked for 3 hours in PBDTx with 2% NGS, and incubated in blocking solution with anti-pH3 antibody (1:300; Upstate Cell Signaling Solutions) overnight at 4°C. After 3 washes in PBDTx for 20 minutes each, embryos were incubated with Alexa568 goat anti-rabbit antibody (1:1000, Molecular Probes) overnight at 4°C and then washed 2 times with PBSTx for 5 minutes each. GFP fluorescence survived both protocols. In order to control for differences in arch area between controls, mutants, and transgenic embryos, Lysotracker- and pH3-positive cells were counted and then divided by arch area to generate cell death and proliferation indexes.

Transplantations

For endoderm transplants, donor *her5*:GFP embryos were injected with Tar* RNA (to promote endoderm targeting) and Rhodamine-Dextran, and cells were transferred to an unlabeled host at 5–6 hpf as described (Crump et al., 2004). Hosts were selected that displayed over 50% contribution of GFP-positive and Rhodamine-positive donor cells to the endoderm anterior to and including the first pouch at 30 hpf. Contralateral sides of the same hosts were used as internal controls, and mutants showing donor tissue only in the trunk were mock transplant controls. Hosts were scored for the severity of Meckel's cartilage loss at 5 days-post-fertilization (dpf).

Imaging and kikGR Photoconversion

Skeletal and colorimetric in situ images were captured on a Leica DM2500 upright microscope. Levels were adjusted using Photoshop CS4 (Adobe) software, with identical adjustments applied throughout the data set. Fluorescent images were acquired on a Zeiss LSM5 inverted confocal microscope using ZEN software. For *sox10*:kikGR photoconversion, the region of interest tool was used to selectively illuminate either the maxillary or mandibular prominence with a 405 nm laser at 50% power for 30 seconds. In order to control for altered arch morphology in mutants and transgenics, we defined the maxillary prominence as anterior to the oral ectoderm and the mandibular prominence as posterior. As the ~4.9 kb *sox10* promoter also results in kikGR expression in chondrocytes, all chondrocytes have green kikGR fluorescence at 5 dpf yet only photoconverted CNCCs

appear red. In order to calculate the areas of arch domains, we first used the 3D tool in the ZEN software to rotate each image into a perfectly lateral aspect and then exported these projections. Using Photoshop we then traced the outline of each domain with the Lasso Tool and recorded total pixels in the Histogram window, followed by conversion to μm^2 using the ZEN-generated scale bar. By extending lines corresponding to the oral ectoderm and first pouch through the DV extent of the arches, we defined maxillary as anterior to oral ectoderm, mandibular as posterior to oral ectoderm and anterior to first pouch, and hyoid as posterior to first pouch.

Statistics

For comparisons of multiple groups, JMP 7.0 software was used for one-way analysis of variance, with a Tukey-Kramer HSD test (α=0.05) showing statistical significance.

RESULTS

spns2 and *s1pr2* mutants display variable gain and/or loss of jaw cartilage elements

In an *N*-ethyl-*N*-nitrosourea mutagenesis screen of 6 dpf zebrafish larvae, the *b1110* allele was isolated based on a disorganized jaw skeleton and cardia bifida. Linkage analysis with dinucleotide-repeat polymorphisms ("Z-markers") placed *b1110* on Linkage Group 5, close to the *spns2* gene whose mutation also results in cardia bifida (Kawahara et al., 2009; Osborne et al., 2008). *b1110* failed to complement the previously reported $spns2^{sk12}$ allele (Osborne et al., 2008), and sequencing of the *spns2* coding sequence in *b1110* revealed an A to T nucleotide change resulting in a premature stop codon after threonine 142. As this mutation is predicted to delete two-thirds of the protein, *b1110* likely corresponds to a complete loss of Spns2 function. As Spns2 functions upstream of the S1pr2 receptor (Kawahara et al., 2009; Osborne et al., 2008), we next analyzed *s1pr2* mutants (Kupperman et al., 2000) and found that they displayed nearly identical craniofacial defects as $spns2^{b1110}$ mutants (Fig. 1). Although cardia bifida and jaw skeletal defects were often seen together, we occasionally observed ectopic jaw skeleton in the absence of heart defects and reciprocally heart defects with a normally patterned jaw (Fig. 1J and Supplementary Fig. 1). Thus, the jaw skeleton defects of $spns2^{b1110}$ and *s1pr2* mutants are not simply an indirect consequence of cardiac defects. However, the higher penetrance of heart defects in *s1pr2* compared to $spns2^{b1110}$ mutants does correlate with the increased penetrance of jaw loss seen in *s1pr2* mutants (Fig. 1I, J).

Whereas the lower jaw skeleton is derived from ventral mandibular CNCCs, the upper jaw skeleton arises from more dorsal maxillary CNCCs (Eberhart et al., 2006). In wild-type larvae at 6 dpf, Meckel's (M) cartilage supports the lower jaw and the pterygoid process (Ptp) of the palatoquadrate (Pq) cartilage the upper jaw, with the upper jaws connecting dorsally to the trabecular (Tr) cartilages of the neurocranium (Fig. 1A). In $spns2^{b1110}$ and *s1pr2* mutants, we observed a phenotypic series of craniofacial defects characterized by ectopic midline cartilage and progressive loss of the normal jaw skeleton, with both ectopic cartilage and jaw reductions occasionally seen in the same animal. In what we refer to as Class 1 mutants (40% of $spns2^{b1110}$ and 28% of *s1pr2* larvae), we observed ectopic cartilage along the ventral midline, either alone (Fig. 1B) or in combination with reduced/disorganized M cartilage (Fig. 1C,G). In contrast, Class 2 mutants displayed only jaw loss, with the lower jaw M cartilage reduced and disorganized in 55% of $spns2^{b1110}$ and 55% of *s1pr2* larvae (Fig. 1D,H) and both M and Pq cartilages lost and the neurocranial Tr and ethmoid cartilages reduced in 2% of $spns2^{b1110}$ and 8% of *s1pr2* larvae (Fig. 1E). Hence, S1P signaling plays a critical role in organizing jaw and neurocranial skeletal development in the anterior head.

Ectopic midline cartilages arise from mandibular CNCCs in *spns2*^{b1110} mutants

We next investigated the developmental origins of ectopic jaw cartilage in Class 1 *spns2*^{b1110} mutants. In order to follow the fate of skeletogenic CNCCs, we created a transgenic line *Tg(sox10:kikGR)*^{el2} in which the photoconvertible kikGR fluorescent protein (Tsutsui et al., 2005) was expressed under the neural-crest-specific *sox10* promoter (Carney et al., 2006). Next, we used ultraviolet light to convert kikGR fluorescence from green to red specifically in the mandibular prominence of 30 hpf wild-type or *spns2*^{b1110} embryos, followed by imaging at 5 dpf to determine the location of red-labeled CNCC derivatives within the larval skeleton (Fig. 1K–M). Consistent with our previous fate maps (Crump et al., 2006), CNCCs of the wild-type mandibular prominence contributed to the lower jaw M cartilage, as well as surrounding mesenchyme, the jaw joint and a portion of Pq (Fig. 1K). In *spns2*^{b1110} embryos, we observed that the mandibular domain was initially disorganized and increased in size at 30 hpf (Fig. 1L,M). As the endodermal and ectodermal epithelia are critical for migrating CNCCs to condense in the arches (Crump et al., 2004; Eberhart et al., 2006), defects in CNCC condensation in *spns2*^{b1110} mutants (due to earlier defects in the anterior endoderm and oral ectoderm - see below) might explain this initial enlargement and disorganization of the mandibular arch. However, by 5 dpf we found that mandibular CNCCs could contribute to either Class 1 ectopic midline cartilage and deformed M cartilage in 33% of *spns2*^{b1110}; *sox10*:kikGR larvae (compare Fig. 1G,L) or Class 2 severe reductions of M cartilage in 67% of cases (compare Fig. 1H,M). Thus, despite an initial enlargement of the mandibular prominence at earlier stages in all *spns2*^{b1110} embryos, mutant mandibular CNCCs can either generate ectopic cartilage or undergo regression and form little or no jaw skeleton.

S1pr2 functions in the endoderm for development of the lower jaw skeleton

The expression patterns of both *spns2* and *s1pr2* are dynamic and complex. At 16 hpf and earlier *spns2* is expressed primarily in the yolk syncitial layer but becomes more widespread by later stages (Kawahara et al., 2009; Osborne et al., 2008), and the receptor gene, *s1pr2*, is expressed in bilateral stripes of mesendoderm until 16 hpf and more clearly in pharyngeal endoderm by 28 hpf (Kupperman et al., 2000). Whereas the expression patterns of these genes do not clearly indicate where they might act, we had previously shown that S1pr2 but not Spns2 is required in the endoderm for heart morphogenesis (Osborne et al., 2008). Hence, we asked here whether S1pr2 also functions in the endoderm for jaw skeletal development. To do so, we transplanted rhodamine-labeled wild-type endoderm precursors into *s1pr2* mutants and scored rescue of the jaw skeleton. In order to control for animal-to-animal variation in *s1pr2* jaw defects (see Fig. 1I), we performed transplants unilaterally, thus allowing us to compare jaw rescue between the transplanted and non-transplanted (control) sides of the same animals. In addition, donor cells harbored an endoderm-specific *her5*:GFP transgene (Tallafuss and Bally-Cuif, 2003) that allowed us to confirm specific targeting of transplanted cells to the endoderm (Fig. 2D,E). Whereas *s1pr2* sides that received wild-type endoderm transplants had a significant improvement in lower jaw development compared to mock transplant controls, non-transplanted control sides showed no improvement (Fig. 2B,C,F). We therefore conclude that S1P signaling functions in the endoderm to promote jaw development, although we cannot rule out that S1P signaling may have additional functions in other arch tissues.

S1P signaling is required for interactions between Shh-expressing endoderm and oral ectoderm

We have previously described that *s1pr2* and *spns2*^{b1110} mutants have disorganization of the pharyngeal endoderm at 18 hpf (Kupperman et al., 2000; Osborne et al., 2008). In addition, avian studies have shown an important role for endoderm-derived Shh in inducing signaling factor expression in the facial ectoderm (Brito et al., 2006; Haworth et al., 2004). We

therefore examined whether the disorganization of the endoderm in *s1pr2* and *spns2*^{b1110} mutants results in abnormal interactions between the Shh-expressing endoderm and facial ectoderm. *pitxc2a* expression marks the oral ectoderm of wild types at 36 hpf (Fig. 3A). In *s1pr2* and *spns2*^{b1110} mutants, as well as in *sox32* mutants that lack endoderm, the *pitxc2a*-expressing oral ectoderm was disorganized and anteriorly displaced (Fig. 3B–D). Reciprocally, the *shha*-expressing pharyngeal endoderm was variably disorganized and/or posteriorly displaced in *s1pr2* and *spns2*^{b1110} mutants and completely absent in *sox32* mutants (Figs 3E–H and 4A–D). In one class of *spns2*^{b1110} mutant (corresponding to Class 2 jaw loss), double fluorescent in situ hybridizations demonstrated that *pitx2ca*-expressing oral ectoderm and *shha*-expressing endoderm failed to make normal contacts (Supplementary Fig. 2). In contrast, in a second class of *s1pr2* mutants (corresponding to Class 1 ectopic jaw), we observed ectopic *shha*-expressing cells anterior to the normal *shha* expression domain (Fig. 4B′,C′). Moreover, the examination of *shhb* expression at 24 hpf (*shhb* is expressed more strongly in the endoderm at this stage than *shha*) similarly revealed both classes of *s1pr2* mutant endodermal defects (posterior displacement and ectopic anterior domains) (Fig. 4E–H). Hence, S1P signaling is required for the morphogenesis of both the pharyngeal endoderm and oral ectoderm, with the variable posterior displacement or ectopic anterior location of Shh-expressing cells consistent with the variable loss or ectopic location of lower jaw skeleton seen in *s1pr2* and *spns2*^{b1110} mutants.

Altered facial ectoderm gene expression in S1P signaling and endoderm mutants

As we found that *s1pr2* and *spns2*^{b1110} mutants have altered interactions between the *shha*-expressing endoderm and oral ectoderm, we next investigated the effects on signaling factor expression within the facial ectoderm. In addition to being expressed in the pharyngeal endoderm, *shha* is also weakly expressed in the oral ectoderm and posterior ectodermal margin (PEM) overlying the second pouch by 36 hpf (Fig. 3E and Supplementary Fig. 3A). Whereas oral ectoderm expression of *shha* was lost in *sox32*, *s1pr2*, and *spns2*^{b1110} mutants (Fig. 3F–H), *shha* expression in the PEM was present in *s1pr2* and *spns2*^{b1110} but not *sox32* mutants (Supplementary Fig. 3B–D). We next examined *fgf8a* expression, as the endoderm and Shh have previously been shown to regulate the ectodermal expression of *Fgf8* in avians (Brito et al., 2008; Haworth et al., 2007). Consistent with the variable reduction or fragmentation of Shh-expressing endoderm in *s1pr2* and *spns2*^{b1110} mutants (Fig. 4A–H), we found that *fgf8a* expression within the oral ectoderm was also variably reduced (Class 2) or fragmented into several loci (Class 1) (Figs 3K,L and 4I–L). In addition, the ectodermal expression of *fgf8a* was greatly reduced in the absence of endoderm in *sox32* mutants (Fig. 3J). Intriguingly, as with the variable disorganization of the *shha*-expressing endoderm, the variable defects in *fgf8a* ectodermal expression in S1P signaling mutants are consistent with the variable loss or gain of jaw cartilage observed. In contrast, *edn1* and *bmp4* were still expressed in the aboral ectoderm (i.e. posterior to the oral ectoderm) in *sox32*, *s1pr2*, and *spns2*^{b1110} embryos, although expression was disorganized and even expanded in some embryos (Fig. 3M–T). As *edn1* and *bmp4* are not exclusively expressed in the ectoderm, the observed expansion of these genes could reflect ectopic expression in other regions of the ectoderm or in other arch tissues. In summary, we conclude that in zebrafish the induction of *fgf8a* and *shha* in the oral ectoderm, but not *edn1* and *bmp4* in the aboral ectoderm, requires signaling from the pharyngeal endoderm.

DV patterning of jaw precursors is largely unaffected in S1P signaling and endoderm mutants

Edn1 and Bmp4 specify ventral fates in mandibular CNCCs that give rise to the lower jaw (Miller et al., 2000; Elizabeth Zuniga and J.G.C., in press), yet our analysis of *sox32* and S1P signaling mutants indicated that the endoderm is not essential for *bmp4* and *edn1* expression in the facial ectoderm. Hence, we analyzed whether the DV specification of jaw

skeletal precursors is also independent of the endoderm. Whereas *dlx2a* was expressed throughout CNCCs of the pharyngeal arches, *hand2* was restricted to ventral, *dlx3b* and *msxe* to DV-intermediate, and *jag1b* to dorsal CNCCs in 36 hpf wild-type embryos (Fig. 5A,E,I,M). Strikingly, *hand2*, *dlx3b*, *msxe*, and *jag1b* transcripts were still largely restricted to their proper DV domains in *sox32*, *s1pr2*, and *spns2*^{b1110} mutants (Fig. 5). However, tracing of expression domains revealed that *hand2* was moderately expanded into the intermediate domain in *s1pr2* and *spns2*^{b1110} mutants (Fig. 5Q), consistent with the variable expansion of *bmp4* and *edn1* expression observed. In addition, *hand2* was ectopically expressed in the posterior second arch ectoderm of *sox32* mutants (arrow in Fig. 5B). Furthermore, tracing of the *dlx2a* expression domains in *s1pr2* and *spns2*^{b1110} mutants showed variable expansion and disorganization of the mandibular arches (Fig. 5Q–T). Hence, S1P signaling and endoderm are required for the proper shape and size, but not the DV identity, of the mandibular arch, consistent with a primary role of endoderm in the growth and/or differentiation of CNCCs as discussed below.

Shha misexpression partially rescues jaw development in endoderm-less *sox32* mutants

We next asked whether transgenic misexpression of Shha could restore jaw skeleton development in the absence of endoderm. These rescue experiments were performed in *sox32* mutants as they display a complete absence of *shha*-expressing endoderm and never form jaw skeleton, as opposed to *s1pr2* and *spns2*^{b1110} mutants that display variably disorganized endoderm and jaw skeleton. To misexpress Shha just prior to pharyngeal arch formation, we first created a *UAS*:Shha transgenic line. In *hsp70I*:Gal4; *UAS*:Shha transgenic embryos subjected to a 14.5–16.5 hpf heat-shock pulse (hereafter referred to as hs-Shha), *shha* expression was upregulated throughout the embryo by 24 hpf (Supplementary Fig. 4I). Importantly, save for a moderate reduction in the overall size of the head skeleton, the transient, embryo-wide Shha misexpression strategy employed did not generally affect craniofacial patterning or embryo development. However, we did observe ectopic cartilages between the upper jaw and neurocranium in hs-Shha larvae (Fig. 6B), similar to what has previously been reported using *shha* mRNA injection (Wada et al., 2005). *sox10*:kikGR fate mapping revealed that these ectopic cartilages were derived from the maxillary domain, which generates the upper jaw (Ptp) and neurocranial trabecular cartilages of wild types (Supplementary Fig. 4A–D). Strikingly, transient induction of Shha from 14.5–16.5 hpf also resulted in substantial recovery of jaw skeleton in *sox32*; hs-Shha larvae compared to *sox32* non-hs-Shha siblings (Fig. 6C,D). Although significantly smaller and dysmorphic compared to their wild-type cognates, lower jaw M and upper jaw Pq cartilages, as well as a small amount of dorsal hyoid cartilage, were identifiable based on their shapes and connectivity (inset Fig. 6H). In contrast, Shha misexpression failed to rescue skeletal development in the ventral hyoid and posterior branchial arches. We thus conclude that Shha is a major endoderm-derived signal for jaw and dorsal hyoid skeletal development.

Shha misexpression restores *fgf8a* expression and arch growth in *sox32* mutants

We next investigated whether the partial rescue of *sox32* jaw defects by Shha correlates with an earlier rescue of ectodermal gene expression. In 36 hpf hs-Shha embryos, we observed a dorsal-anterior shift of *fgf8a* oral ectoderm expression (Fig. 6F), and *pitxc2a* labeling revealed that this shift was likely due to abnormal positioning of the oral ectoderm (Supplementary Fig. 4J). In contrast, the ectodermal expression of *edn1* and *bmp4* were largely unaffected in hs-Shha embryos (Supplementary Fig. 4K,L). In addition, we found that Shha misexpression rescued the *fgf8a* expression defects of *sox32* mutants, with the recovered *fgf8a* expression being dorsal-anterior-shifted as in hs-Shha embryos (Fig. 6H). Next, we analyzed the cellular mechanisms by which Shha misexpression rescues jaw development in *sox32* mutants. In control 30 hpf embryos, the *fli1a*:GFP transgene (Lawson

and Weinstein, 2002) labels CNCCs of the mandibular, hyoid, and more posterior branchial arches (Fig. 6I). In hs-Shha; *fli1a*:GFP embryos the maxillary domain of the mandibular arch (which generates the upper jaw and part of the neurocranium) was increased in size (Fig. 6J,U). Whereas the maxillary and mandibular domains of the mandibular arch, as well as the hyoid arch, were smaller in *sox32* embryos, Shha misexpression restored the size of both the mandibular and hyoid arches (Fig. 6K,L,U). We next performed proliferation (anti-pH3) and cell death (Lyostracker) assays to determine how Shha rescues arch size in *sox32* mutants. Whereas hs-Shha and *sox32* mutant embryos did not have significant differences in proliferation from controls, Shha misexpression increased the cell proliferation index of *sox32* mutant *fli1a*:GFP^{+} CNCCs in the mandibular arch (Fig. 6M–P,U). In addition, as previously reported using Acridine Orange and TUNEL staining (David et al., 2002), we found an increase in LysoTracker^{+} *fli1a*:GFP^{+} CNCCs in the mandibular and hyoid arches of *sox32* mutants, with Shha misexpression rescuing cell death in the hyoid arch (Fig. 6Q–U). Together, our data suggest that a major role of endoderm-derived Shh is to induce *fgf8a* expression in the oral ectoderm, with Shha and Fgf8a promoting the proliferation and survival of facial skeletal precursors.

DISCUSSION

Here we describe a new role for the S1P signaling proteins, Spns2 and S1pr2, in development of the jaw skeleton. In particular, we demonstrate that S1P signaling acts indirectly in jaw development by controlling the morphogenesis of the anterior-most Shh-expressing endoderm underlying the mandibular arch. As such, Spns2 and S1pr2 represent new candidate genes for craniofacial birth defects that affect the jaw and skull. Moreover, our genetic analysis reveals that the anterior pharyngeal endoderm promotes the growth and/or differentiation yet is largely dispensable for the DV patterning of jaw skeletal precursors (Fig. 7A).

S1P functions in the anterior pharyngeal endoderm to regulate facial ectoderm gene expression and jaw development

We had previously reported that Integrinα5 is required in more posterior endoderm for development of the first pharyngeal pouch, with loss of the first endodermal pouch resulting in specific defects in hyoid-arch-derived skeleton (Crump et al., 2004). Here our analysis of S1P signaling mutants reveals a specific requirement of the anterior-most endoderm in development of the mandibular-arch-derived jaw and neurocranial skeleton. S1P signaling appears to function primarily in the endoderm for lower jaw development, as we can partially rescue *s1pr2* jaw defects with wild-type endoderm transplants. The lack of full rescue might be due to our inability to completely repopulate *sr1p2* mutant embryos with wild-type endoderm, or it could be that S1P signaling has additional roles in other arch tissues. As S1P signaling mutants have no defects in pouch endoderm, our results suggest a distinct role for S1P signaling in morphogenesis of the anterior endoderm underlying the mandibular arch. We have previously reported that Spns2 acts in the yolk syncytial layer to promote the export of S1P, which then acts on overlying S1pr2-expressing endoderm cells (Kawahara et al., 2009; Osborne et al., 2008). Whereas the mechanism by which S1P signaling controls endoderm morphogenesis requires further investigation, S1P signaling might control either the adhesion or movements of early anterior endodermal cells, with a failure in these processes resulting in abnormal contacts between the Shh-expressing endoderm and oral ectoderm.

Similar to the results of avian studies (Brito et al., 2008; Haworth et al., 2007), we find that Shh from the endoderm promotes Fgf8 expression in the facial ectoderm of zebrafish. Hence, the variable disorganization of *fgf8a* expression resulting from abnormal contacts between ectopic Shh-expressing endoderm and facial ectoderm might explain the ectopic

jaw skeleton observed in less severe S1P signaling mutants (Fig. 7C). In more severe S1P signaling mutants and *sox32* mutants that lack endoderm, a failure of Shh-expressing endoderm cells to contact the ectoderm would result in an absence of ectodermal *fgf8a* expression and subsequent jaw loss (Fig. 7D,E). Moreover, jaw defects in S1P signaling mutants might be due to both altered gene expression within the oral ectoderm and defective morphogenesis of the oral ectoderm. Indeed, interactions between the pharyngeal endoderm and oral ectoderm are important for the cellular rearrangements that form the anterior opening of the gut tube, the primary mouth (Dickinson and Sive, 2006). As the oral ectoderm of S1P signaling and *sox32* mutants does not extend as posteriorly as in wild types, our results suggest that the endoderm is also required for the proper posterior extension of the oral ectoderm.

Endoderm is required for the growth but not the DV identity of jaw precursors

In general, our genetic findings in zebrafish agree with surgical experiments in avians demonstrating that distinct domains of pharyngeal endoderm are required for the development of specific facial skeletal elements (Couly et al., 2002; Ruhin et al., 2003). However, rather than specifying the regional identity of skeletal elements per se, our data suggest that the endoderm is primarily involved in the selective growth and/or differentiation of pre-specified skeletal precursors. In endoderm-less *sox32* mutants the facial skeleton is completely lost, yet we find that at the level of gene expression facial skeletal precursors still acquire largely normal DV identity. Consistent with DV patterning of CNCCs being unaffected by loss of endoderm, we find that the important DV signaling molecules, Bmp4 and Edn1, are still expressed in *sox32* and S1P signaling mutants. Our results are somewhat different than those of avian studies that found a role for endoderm in inducing *Bmp4* expression in the facial ectoderm (Brito et al., 2006, 2008). The apparent species-specific differences in *bmp4* regulation could be explained by the more precise genetic ablation of endoderm used here, or could reflect real differences in gene regulation between avians and fish. On the other hand, we find that the role of the Shh-expressing endoderm in inducing *fgf8a* expression in the oral ectoderm is conserved between zebrafish and avians. In zebrafish, *fgf8a* oral ectoderm expression is greatly reduced when the Shh-expressing endoderm is missing in *sox32* mutants, with *fgf8a* expression restored by Shha misexpression. However, some *fgf8a* expression persists even in the complete absence of endoderm (e.g. Figs 3J and 6G), consistent with reports in zebrafish that Shh from the ventral brain also regulates *fgf8a* expression in the oral ectoderm (Eberhart et al., 2006). Furthermore, our data implicate Shh and Fgf8 signaling in the growth of jaw skeletal precursors, as Shha misexpression rescues *fgf8a* expression, arch size, and CNCC proliferation and survival in *sox32* mutants. This is consistent with previous results showing that Shh and Fgf signaling promote both the proliferation and survival of skeletogenic CNCCs (David et al., 2002; Jeong et al., 2004; Trumpp et al., 1999). However, despite the ability of Shh misexpression to rescue arch size in the absence of endoderm, later jaw skeleton is only weakly restored. The lack of full skeletal rescue might reflect additional endodermal signals required for skeletal development or continuous requirements for Shh in CNCC survival, proliferation, and/or differentiation. Indeed, the analysis of Shh signaling mutants in zebrafish suggests that endoderm-derived Shh also plays a role in the differentiation of CNCCs into cartilage (Schwend and Ahlgren, 2009), and hence “rescued” *sox32* mutant CNCCs may not efficiently differentiate into cartilage due to the early pulse of Shha protein not perduring at later stages.

Although we find that the endoderm is dispensable for the DV identity of jaw precursors, our results in zebrafish are not at odds with previous avian studies showing that endodermal grafts from distinct domains induced supernumerary skeletal elements of a particular type and orientation (Couly et al., 2002; Ruhin et al., 2003). In those studies, endodermal grafts

were not able to reprogram the regional identity of existing skeletal precursors but instead increased the growth of a particular domain such that multiple elements of the same type developed, with the polarized expression of growth factors within these endodermal grafts likely directing the orientation of these supernumerary elements. In other words, the results of both avian grafting experiments and our genetics studies in zebrafish suggest that particular skeletal precursor domains are not initially specified by the endoderm but may be uniquely responsive to distinct endodermal domains for their directional growth.

During vertebrate evolution, changes in the levels and location of epithelial signaling molecules have been proposed to result in differential growth of facial prominences and concomitant craniofacial diversification (Shigetani et al., 2002; Wu et al., 2004). Interestingly, the ectopic mandibular cartilages we observe in S1P signaling mutants bear a striking resemblance to the basimandibular midline cartilages reported in dogfish (El-Toubi, 1949) and the Australian lungfish (see Fig. 4 in (Bartsch, 1994)). Hence, we propose that variations in endoderm-ectoderm interactions, analogous to what occurs in S1P signaling mutants with altered endoderm morphogenesis, might lead to increased growth of particular domains and the concomitant formation of new facial skeletal elements during vertebrate radiation.

Supplementary Material

Refer to Web version on PubMed Central for supplementary material.

Acknowledgments

We thank Corey Gingerich for fish care and Abigail Tucker and Francesca Mariani for helpful comments. Research was supported by NIH grants DE018405 and DE018405-03S1 to J.G.C. and HL54737 to D.Y.R.S. NIH grants DE13834 and HD22486 funded the University of Oregon skeletal screen.

References

Alexander J, Rothenberg M, Henry GL, Stainier DY. casanova plays an early and essential role in endoderm formation in zebrafish. Dev Biol. 1999; 215:343–357. [PubMed: 10545242]

Barlow AJ, Francis-West PH. Ectopic application of recombinant BMP-2 and BMP-4 can change patterning of developing chick facial primordia. Development. 1997; 124:391–398. [PubMed: 9053315]

Bartsch P. Development of the cranium of *Neoceratodus forsteri*, with a discussion of the suspensorium and the opercular apparatus in Dipnoi. Zoomorphology. 1994; 114:1–31.

Brito JM, Teillet MA, Le Douarin NM. An early role for sonic hedgehog from foregut endoderm in jaw development: ensuring neural crest cell survival. Proc Natl Acad Sci U S A. 2006; 103:11607–11612. [PubMed: 16868080]

Brito JM, Teillet MA, Le Douarin NM. Induction of mirror-image supernumerary jaws in chicken mandibular mesenchyme by Sonic Hedgehog-producing cells. Development. 2008; 135:2311–2319. [PubMed: 18539924]

Carney TJ, Dutton KA, Greenhill E, Delfino-Machin M, Dufourcq P, Blader P, Kelsh RN. A direct role for Sox10 in specification of neural crest-derived sensory neurons. Development. 2006; 133:4619–4630. [PubMed: 17065232]

Couly G, Creuzet S, Bennaceur S, Vincent C, Le Douarin NM. Interactions between Hox-negative cephalic neural crest cells and the foregut endoderm in patterning the facial skeleton in the vertebrate head. Development. 2002; 129:1061–1073. [PubMed: 11861488]

Crump JG, Swartz ME, Eberhart JK, Kimmel CB. Moz-dependent Hox expression controls segment-specific fate maps of skeletal precursors in the face. Development. 2006; 133:2661–2669. [PubMed: 16774997]

Crump JG, Swartz ME, Kimmel CB. An Integrin-Dependent Role of Pouch Endoderm in Hyoid Cartilage Development. PLoS Biol. 2004; 2:E244. [PubMed: 15269787]

David NB, Saint-Etienne L, Tsang M, Schilling TF, Rosa FM. Requirement for endoderm and FGF3 in ventral head skeleton formation. Development. 2002; 129:4457–4468. [PubMed: 12223404]

Dickinson AJ, Sive H. Development of the primary mouth in Xenopus laevis. Dev Biol. 2006; 295:700–713. [PubMed: 16678148]

Eberhart JK, Swartz ME, Crump JG, Kimmel CB. Early Hedgehog signaling from neural to oral epithelium organizes anterior craniofacial development. Development. 2006; 133:1069–1077. [PubMed: 16481351]

El-Toubi MR. The development of the chondrocranium of the spiny dogfish, Acanthias vulgaris (Squalus acanthias) neurocranium, mandibular and hyoid arches. J Morphol. 1949; 84:227–279. [PubMed: 18116895]

Epperlein HH, Lehmann R. The ectomesenchymal-endodermal interaction-system (EEIS) of Triturus alpestris in tissue culture. I. Observations on the differentiation of visceral cartilage. Differentiation. 1975; 4:159–174.

Haworth KE, Healy C, Morgan P, Sharpe PT. Regionalisation of early head ectoderm is regulated by endoderm and prepatterns the orofacial epithelium. Development. 2004; 131:4797–4806. [PubMed: 15342462]

Haworth KE, Wilson JM, Grevellec A, Cobourne MT, Healy C, Helms JA, Sharpe PT, Tucker AS. Sonic hedgehog in the pharyngeal endoderm controls arch pattern via regulation of Fgf8 in head ectoderm. Dev Biol. 2007; 303:244–258. [PubMed: 17187772]

Jeong J, Mao J, Tenzen T, Kottmann AH, McMahon AP. Hedgehog signaling in the neural crest cells regulates the patterning and growth of facial primordia. Genes Dev. 2004; 18:937–951. [PubMed: 15107405]

Kawahara A, Nishi T, Hisano Y, Fukui H, Yamaguchi A, Mochizuki N. The sphingolipid transporter spns2 functions in migration of zebrafish myocardial precursors. Science. 2009; 323:524–527. [PubMed: 19074308]

Kikuchi Y, Agathon A, Alexander J, Thisse C, Waldron S, Yelon D, Thisse B, Stainier DY. casanova encodes a novel Sox-related protein necessary and sufficient for early endoderm formation in zebrafish. Genes Dev. 2001; 15:1493–1505. [PubMed: 11410530]

Kupperman E, An S, Osborne N, Waldron S, Stainier DY. A sphingosine-1-phosphate receptor regulates cell migration during vertebrate heart development. Nature. 2000; 406:192–195. [PubMed: 10910360]

Kurihara Y, Kurihara H, Suzuki H, Kodama T, Maemura K, Nagai R, Oda H, Kuwaki T, Cao WH, Kamada N, et al. Elevated blood pressure and craniofacial abnormalities in mice deficient in endothelin-1. Nature. 1994; 368:703–710. [PubMed: 8152482]

Kwan KM, Fujimoto E, Grabher C, Mangum BD, Hardy ME, Campbell DS, Parant JM, Yost HJ, Kanki JP, Chien CB. The Tol2kit: a multisite gateway-based construction kit for Tol2 transposon transgenesis constructs. Dev Dyn. 2007; 236:3088–3099. [PubMed: 17937395]

Lawson ND, Weinstein BM. In vivo imaging of embryonic vascular development using transgenic zebrafish. Dev Biol. 2002; 248:307–318. [PubMed: 12167406]

Liu W, Selever J, Murali D, Sun X, Brugger SM, Ma L, Schwartz RJ, Maxson R, Furuta Y, Martin JF. Threshold-specific requirements for Bmp4 in mandibular development. Dev Biol. 2005; 283:282–293. [PubMed: 15936012]

Maves L, Jackman W, Kimmel CB. FGF3 and FGF8 mediate a rhombomere 4 signaling activity in the zebrafish hindbrain. Development. 2002; 129:3825–3837. [PubMed: 12135921]

Miller CT, Maves L, Kimmel CB. moz regulates Hox expression and pharyngeal segmental identity in zebrafish. Development. 2004; 131:2443–2461. [PubMed: 15128673]

Miller CT, Schilling TF, Lee K, Parker J, Kimmel CB. sucker encodes a zebrafish Endothelin-1 required for ventral pharyngeal arch development. Development. 2000; 127:3815–3828. [PubMed: 10934026]

Nair S, Li W, Cornell R, Schilling TF. Requirements for Endothelin type-A receptors and Endothelin-1 signaling in the facial ectoderm for the patterning of skeletogenic neural crest cells in zebrafish. Development. 2007; 134:335–345. [PubMed: 17166927]

Osborne N, Brand-Arzamendi K, Ober EA, Jin SW, Verkade H, Holtzman NG, Yelon D, Stainier DY. The spinster homolog, two of hearts, is required for sphingosine 1-phosphate signaling in zebrafish. Curr Biol. 2008; 18:1882–1888. [PubMed: 19062281]

Ruhin B, Creuzet S, Vincent C, Benouaiche L, Le Douarin NM, Couly G. Patterning of the hyoid cartilage depends upon signals arising from the ventral foregut endoderm. Dev Dyn. 2003; 228:239–246. [PubMed: 14517995]

Scheer N, Campos-Ortega JA. Use of the Gal4-UAS technique for targeted gene expression in the zebrafish. Mech Dev. 1999; 80:153–158. [PubMed: 10072782]

Schwend T, Ahlgren SC. Zebrafish con/disp1 reveals multiple spatiotemporal requirements for Hedgehog-signaling in craniofacial development. BMC Dev Biol. 2009; 9:59. [PubMed: 19948063]

Shigetani Y, Sugahara F, Kawakami Y, Murakami Y, Hirano S, Kuratani S. Heterotopic shift of epithelial-mesenchymal interactions in vertebrate jaw evolution. Science. 2002; 296:1316–1319. [PubMed: 12016315]

Spiegel S, English D, Milstien S. Sphingosine 1-phosphate signaling: providing cells with a sense of direction. Trends Cell Biol. 2002; 12:236–242. [PubMed: 12062172]

Tallafuss A, Bally-Cuif L. Tracing of her5 progeny in zebrafish transgenics reveals the dynamics of midbrain-hindbrain neurogenesis and maintenance. Development. 2003; 130:4307–4323. [PubMed: 12900448]

Trumpp A, Depew MJ, Rubenstein JL, Bishop JM, Martin GR. Cre-mediated gene inactivation demonstrates that FGF8 is required for cell survival and patterning of the first branchial arch. Genes Dev. 1999; 13:3136–3148. [PubMed: 10601039]

Tsutsui H, Karasawa S, Shimizu H, Nukina N, Miyawaki A. Semi-rational engineering of a coral fluorescent protein into an efficient highlighter. EMBO Rep. 2005; 6:233–238. [PubMed: 15731765]

Tucker AS, Yamada G, Grigoriou M, Pachnis V, Sharpe PT. Fgf-8 determines rostral-caudal polarity in the first branchial arch. Development. 1999; 126:51–61. [PubMed: 9834185]

Wada N, Javidan Y, Nelson S, Carney TJ, Kelsh RN, Schilling TF. Hedgehog signaling is required for cranial neural crest morphogenesis and chondrogenesis at the midline in the zebrafish skull. Development. 2005; 132:3977–3988. [PubMed: 16049113]

Walker MB, Kimmel CB. A two-color acid-free cartilage and bone stain for zebrafish larvae. Biotech Histochem. 2007; 82:23–28. [PubMed: 17510811]

Wu P, Jiang TX, Suksaweang S, Widelitz RB, Chuong CM. Molecular shaping of the beak. Science. 2004; 305:1465–1466. [PubMed: 15353803]

Zuniga E, Stellabotte F, Crump JG. Jagged-Notch signaling ensures dorsal skeletal identity in the vertebrate face. Development. 2010; 137:1843–1852. [PubMed: 20431122]

HIGHLIGHTS

- Novel role of Sphingosine-1-phosphate signaling in jaw development
- Sphingosine-1-phosphate signaling functions in the endoderm to organize mandibular arch growth
- Endoderm is dispensable for dorsoventral patterning of upper versus lower jaw precursors
- Reintroduction of Shh can partially rescues jaw development in the genetic absence of endoderm

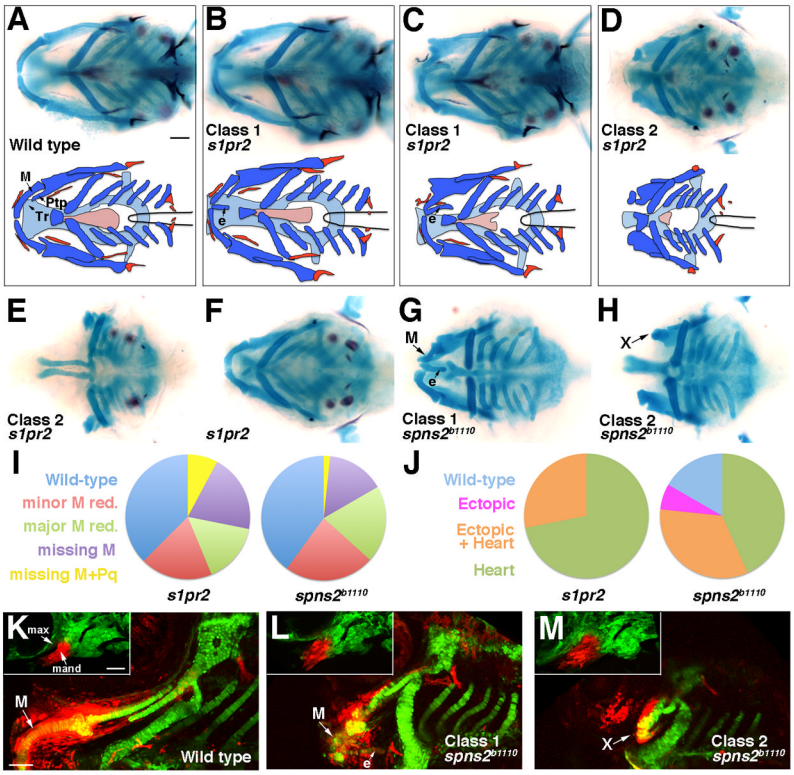

Figure 1. Jaw skeletal defects in *s1pr2* and *spns2*^{b1110} mutants

(**A–H**) Ventral views show head skeletons of 6 dpf zebrafish larvae stained for cartilage (blue) and bone (red) in (A–F) and cartilage only in (G, H). Bottom schematics in (A–D) show facial cartilage (dark blue), neurocranial cartilage (light blue), and bone and teeth (red). Meckel's (M), pterygoid process (Ptp), and trabecular (Tr) cartilages are indicated. *s1pr2* and *spns2*^{b1110} larvae variably displayed ectopic (e) midline cartilage (Class 1: B, C, G) and/or graded reductions of jaw and anterior neurocranial skeleton (Class 2: D, E, H). In addition, some genotypically mutant *s1pr2* and *spns2*^{b1110} larvae displayed a normally patterned jaw (F).

(**I** and **J**) Pie charts show proportions of *s1pr2* (n = 32) and *spns2*^{b1110} (n = 30) larvae showing progressive reductions of jaw skeleton (I, scored for each side) and ectopic cartilage and/or heart defects (J, scored for each animal). Minor M reduction refers to losses of less than 50% of the cartilage (e.g. C, G) and major M reduction losses greater than 50% (e.g. top of D). More severe categories include missing M (e.g. bottom D) and missing M + Pq (e.g. E). Wild-type siblings never displayed defects.

(**K–M**) *sox10*:kikGR imaging of the mandibular and hyoid arches at 30 hpf (insets) and the resulting skeletal derivatives at 5 dpf. Photoconversion of mandibular (mand) prominence CNCCs (red) resulted in labeling of Meckel's (M) cartilage and surrounding mesenchyme in wild types (n = 3/3). In *spns2*^{b1110}; *sox10*:kikGR larvae, mandibular CNCCs generated either malformed M and ectopic (e) midline cartilages (L, n = 3/9) or very reduced remnants ("X") (M, n = 6/9). Max, maxillary prominence. Scale bars = 50 μm.

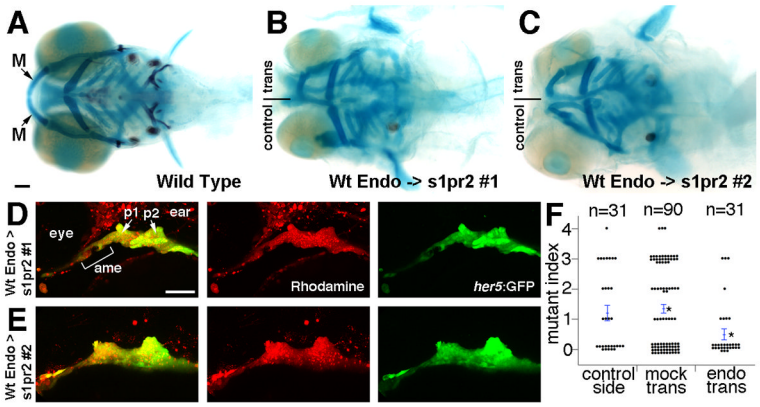

Figure 2. Wild-type endoderm rescues lower jaw development in *s1pr2* mutants

(**A–C**) Ventral views of 6 dpf head skeletons. Unilateral transplantation of wild-type endoderm precursors into *s1pr2* mutants rescued the loss (B) or reduction (C) of lower jaw M cartilage seen in control sides not receiving transplants.

(D and **E)** The same two examples imaged at 30 hpf to show the contribution of wild-type *her5*:GFP^{+} (green) rhodamine-dextran^{+} (red) donor endoderm cells to the anterior medial endoderm (ame) and the first and second pouches (p1 and p2) of the host arches.

(F) For quantification of lower jaw rescue, we devised a mutant index: 0, wild type; 1, minor M reduction; 2, major M reduction; 3, M missing; 4, M and Pq missing. Compared to *s1pr2* mutants receiving mock transplants, mutant sides receiving endoderm transplants (but not the contralateral control sides of the same animals) had partial restoration of lower jaw cartilage. Individual data points are plotted, and bars show standard error of the mean. Asterisks denote the two groups with statistical differences in average jaw skeleton defects. Scale bars = 50 μm.

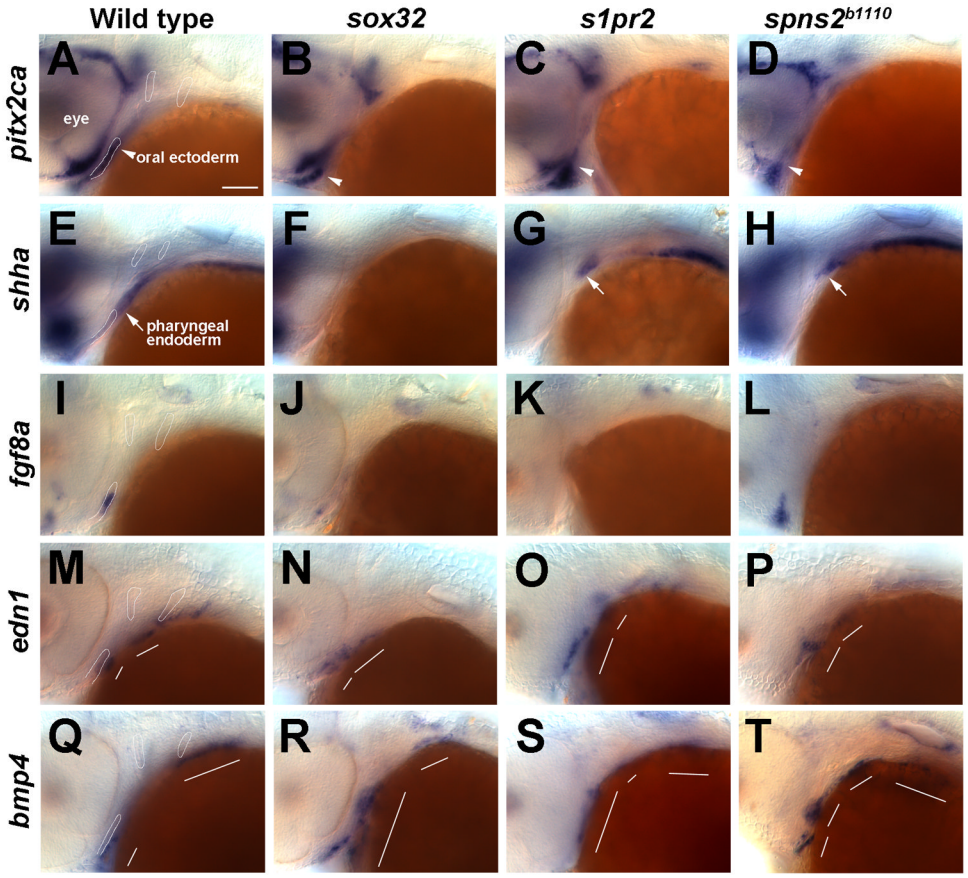

Figure 3. Facial ectoderm gene expression in endoderm mutants

(**A–T**) In situ hybridizations at 36 hpf. In wild types, *pitx2ca* (A), *shha* (E), and *fgf8a* (I) are expressed in oral ectoderm and *edn1* (M) and *bmp4* (Q) in aboral ectoderm. *pitx2ca* expression in the oral ectoderm (arrowheads) is present but shifted anteriorly in *sox32* (B, n = 6/6), *s1pr2* (C, n = 11/11), and *spns2*^{b1110} (D, n = 4/4) embryos. The expression of *shha* in the oral ectoderm is lost in all mutants, whereas endoderm expression (arrows) is absent in *sox32* mutants (F, n = 7/7), variably posteriorly displaced (G, n = 10/15) or disorganized (see Fig. 4, n = 3/15) in *s1pr2* mutants, and variably posteriorly displaced (H, n = 6/7) or disorganized (not shown, n = 1/7) in *spns2*^{b1110} mutants. *fgf8a* expression is reduced in *sox32* mutants (J, n = 6/6), reduced (K, n= 4/10) or disorganized (not shown, n= 4/10) in *s1pr2* mutants, and reduced (not shown, n= 13/27) or disorganized (L, n= 14/27) in *spns2*^{b1110} mutants. *edn1* expression in the first two arches (white lines) is present but disorganized in *sox32* (N, n = 8/8), *s1pr2* (O, n = 6/6), and *spns2*^{b1110} (P, n = 5/5) mutants. *bmp4* expression is also disorganized in *sox32* (R, n = 6/6), *s1pr2* (S, n = 7/7), and *spns2*^{b1110} (T, n = 5/5) mutants. Outlines of the oral ectoderm and first two pouches are shown for wild types. Scale bar = 50 μm.

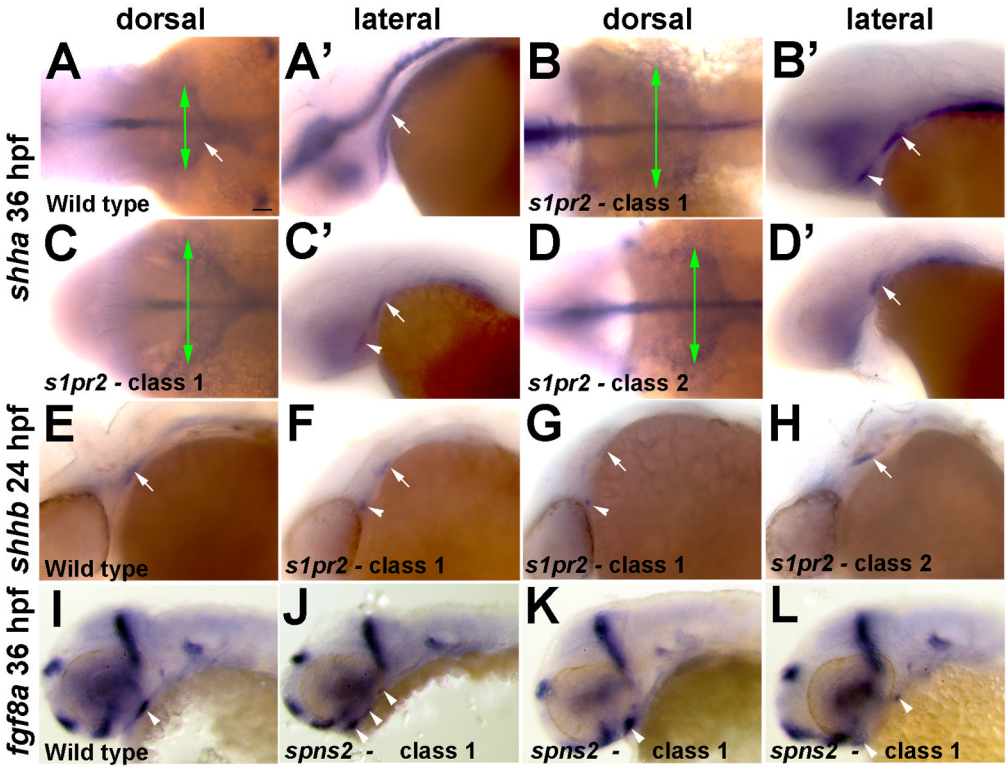

Figure 4. Variable disorganization of Shh-expressing endoderm and *fgf8a* ectodermal expression in *s1pr2* and *spns2*^{b1110} mutants

(**A–D**) In situ hybridizations at 36 hpf show two classes of *shha* expression in *s1pr2* mutants. When viewed dorsally Class 1 mutants have a wider *shha* endodermal expression domain (green arrows) than Class 2 mutants, and in lateral views of the same embryos Class 1 but not Class 2 mutants display ectopic *shha* expression (arrowheads) anterior to the normal expression domains (arrows).

(**E–H)** In situ hybridizations at 24 hpf also show two classes of *shhb* expression in *s1pr2* mutants, with Class I mutants (n = 3/8) showing ectopic anterior expression and Class 2 mutants (n = 5/8) displaying posterior truncation of the normal endodermal expression domain (arrows).

(**I–F)** Several examples of *spns2*^{b1110} Class I mutants show fragmented expression of *fgf8a* expression in the oral ectoderm (arrowheads). Scale bar = 50 μm.

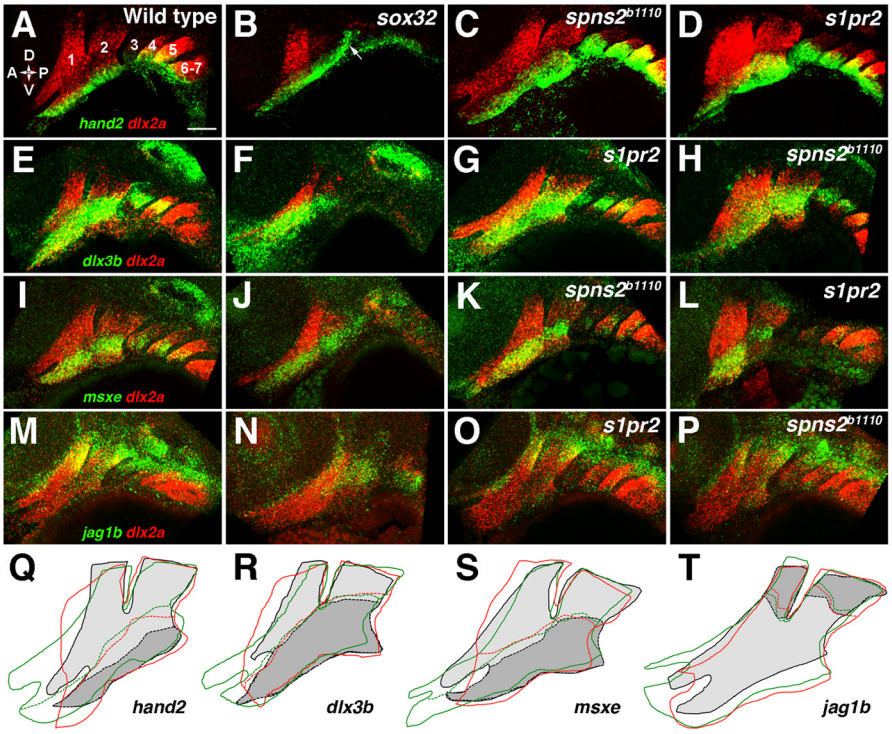

Figure 5. DV gene expression in endoderm mutants

(**A–P**) Double fluorescent in situ hybridizations show the expression of *dlx2a* (red) with *hand2*, *dlx3b*, *msxe*, or *jag1b* (green) in the pharyngeal arches (numbered) at 36 hpf. In wild types, *hand2* (A) was restricted to the ventral-most domain, *dlx3b* (E) and *msxe* (I) to a DV-intermediate domain, and *jag1b* (M) to the dorsal arches. *hand2* expression remained restricted to ventral arch CNCCs in *sox32* embryos, although ectopic *hand2* expression was seen in ectoderm overlying the second pouch (arrow) (B, n = 12/12). The *hand2* expression domain remained ventrally restricted but was expanded in size in *s1pr2* (D, n = 10/10), and *spns2*^{b1110} (C, n = 10/10) embryos. The DV-intermediate expression of *dlx3b* was normal in *sox32* (F, n = 4/4), *s1pr2* (G, n = 10/10), and *spns2*^{b1110} (H, n = 5/5) embryos, as was expression of *msxe* in *sox32* (J, n = 7/7), *s1pr2* (L, n = 11/11), and *spns2*^{b1110} (K, n = 5/5) embryos. *jag1b* expression was reduced but remained dorsal-restricted in *sox32* embryos (N, n = 5/5) and was unaffected in *s1pr2* (O, n = 5/5) and *spns2*^{b1110} (P, n = 6/6) embryos. (**Q–T**) Tracings of the *dlx2a*-expressing arches (solid lines) and the DV expression borders (dashed lines) of *hand2* (Q), *dlx3b* (R), *msxe* (S), or *jag1b* (T) show slight expansion of *hand2* expression but no change in *dlx3b*, *msxe*, or *jag1b* expression in two classes of *s1pr2* and *spns2*^{b1110} mutants. For wild types, *dlx2a* expression is light gray, with DV gene expression domains in darker gray. The mandibular arch was expanded (green lines) in some embryos (C,G,K,O; 47% of *s1pr2* and 53% of *spns2*^{b1110}) and was abnormally shaped and/or anteriorly truncated (red lines) in other embryos (D,H,L,P; 47% of *s1pr2* and 16% of *spns2*^{b1110}). Scale bar = 50 μm.

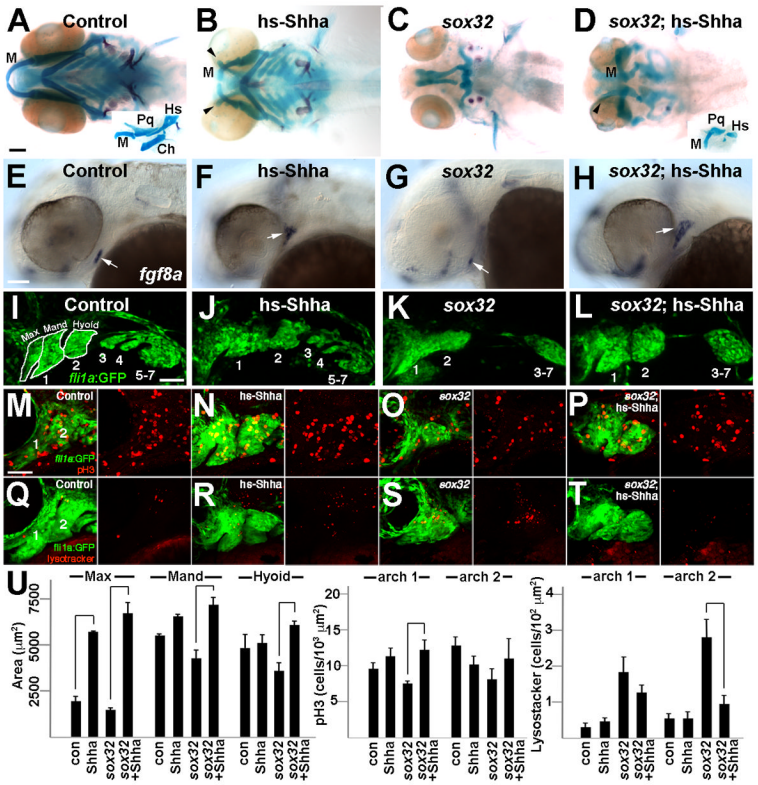

Figure 6. Shha misexpression partially rescues the jaw defects of *sox32* mutants

(**A–D**) Ventral views of 6 dpf head skeletons. Compared to *hsp70I*:Gal4 controls subjected to the same heat-shock treatment (A), hs-Shha larvae developed ectopic Tr-like cartilages (arrowheads) (B, n = 10/10). Whereas facial skeleton never formed in non-hs-Shha *sox32* siblings (C, n = 0/10), jaw and hyoid cartilage was partially restored and ectopic cartilage was still present in *sox32*; hs-Shha larvae (D, n = 4/4). Flat-mount preparations (insets in A and D) show that Meckel's (M), palatoquadrate (Pq), and hyosymplectic (Hs) cartilages, but not the hyoid-arch-derived ceratohyal (Ch) cartilage, were dysmorphic yet present in *sox32*; hs-Shha larvae.

(E–F) In situ hybridizations show *fgf8a* oral ectoderm expression (arrows) at 36 hpf. Compared to *hsp70I*:Gal4 controls (E), *fgf8* expression was shifted dorsal-anteriorly in hs-Shha embryos (F, n = 8/9) and partially (n = 3/34) or severely reduced (n = 31/34) in *sox32* mutants (G). Shha misexpression resulted in increased and dorsal-laterally shifted *fgf8a* expression in *sox32*; hs-Shha embryos (H, n = 11/12).

(I–L) Confocal projections show the pharyngeal arches (numbered) of control *fli1a*:GFP (I, n = 3), hs-Shha; *fli1a*:GFP (J, n = 4), *sox32; fli1a*:GFP (K, n = 10), and *sox32*; hs-Shha; *fli1a*:GFP (L, n = 7) embryos at 30 hpf. In *sox32* and *sox32*; hs-Shha embryos, the lack of endoderm resulted in arches 3–7 remaining as a single mass. White outlines show the maxillary (max), mandibular (mand), and hyoid domains for wild type.

(M–T) Anti-pH3 staining marks proliferating cells (red, M-P), Lysotracker marks regions of cell death (red, Q-T), and *fli1a*:GFP labels CNCCs (green) of the mandibular (1) and hyoid (2) arches in control (M and Q), hs-Shha (N and R), *sox32* (O and S), and *sox32*; hs-Shha (P and T) embryos at 36 hpf. n = 10 for each genotype. Scale bars = 50 μm.

(**U**) Quantification of arch domain area and numbers of pH3- and Lysotracker-positive cells per arch area in control *hsp70I*:Gal4 (con), hs-Shha, *sox32*, and *sox32*; hs-Shha embryos. Brackets indicate comparisons showing statistical significance with a Tukey-Kramer HSD test (α=0.05).

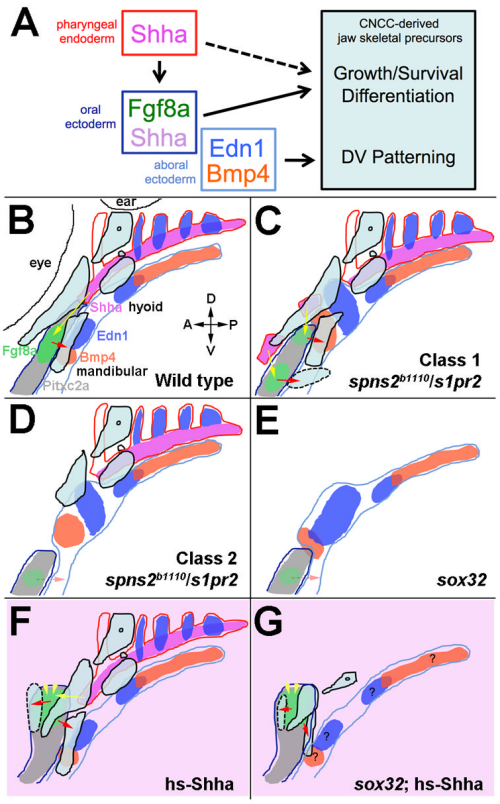

Figure 7. Model of tissue-tissue interactions during facial skeleton development

(A) Endodermal Shha induces *fgf8a* and *shha* expression in the oral ectoderm. Whereas ectodermal Fgf8a and/or Shha promote the growth and/or differentiation of jaw skeletal precursors, an endoderm-independent Edn1 and Bmp4 signaling center in the aboral ectoderm regulates the DV patterning of jaw precursors. Endoderm may also have direct effects on skeletal growth and/or differentiation.

(B) Schematic of the wild-type arches shows gene expression in the pharyngeal endoderm (red outlines), oral ectoderm (dark blue outlines), and aboral ectoderm (light blue outlines), as well as mandibular- and hyoid-arch-derived cartilage precursors (black outlines with light blue fill) at 36 hpf. *fgf8a* (green) is expressed within the *pitxc2a*-positive (grey) oral ectoderm, and *bmp4* (orange) and *edn1* (blue) are expressed within the aboral ectoderm and pouch endoderm. *shha* (pink) is expressed in the medial pharyngeal endoderm (and weakly in the oral ectoderm, not shown). Shha signaling (yellow arrow) promotes *fgf8a* expression, with Fgf8a signaling (red arrow) regulating the position of the lower jaw skeleton.

(**C**–**E**) In *spns2*^{b1110}, *s1pr2*, and *sox32* mutants, disorganization and/or loss of the pharyngeal endoderm results in altered gene expression within the oral and aboral ectoderm. In Class I S1P mutants, altered morphogenesis of Shha-expressing endoderm cells induces ectopic *fgf8a* expression in the oral ectoderm and the induction of ectopic midline cartilage (dotted line). In class 2 S1P and *sox32* mutants, loss of anterior endoderm results in reduction of *fgf8a* expression, posterior truncation of the oral ectoderm, and loss of jaw skeleton.

(**F** and **G**) Transient embryo-wide Shha misexpression (light pink) results in increased Shha signaling (yellow arrowheads), dorsal-lateral displacement of *fgf8a* and the *pitxc2a*-expressing oral ectoderm, and the formation of ectopic maxillary cartilage (dotted line). Shha misexpression in *sox32* mutants restores *fgf8a* expression and partially rescues jaw skeleton development.